# The development of a continuum framework for friction welding processes with the aid of micro-mechanical parameterisations

Achilles Vairis*

Centre for Technological Research – Crete,
P.O. Box 1939, Heraklion 71004, Greece
E-mail: vairis@stef.teiher.gr
*Corresponding author

Nicholas Christakis

Department of Applied Mathematics,
University of Crete,
Heraklion 71409, Greece
E-mail: nicholas.christakis@physics.org

**Abstract:** Continuum modelling of complex industrial systems can be addressed with the aid of micromechanical parameterisations. The appropriate framework has been demonstrated through recent work in the area of modelling complex industrial processes which involve granular material. In this paper, the framework is set for the continuum modelling of friction welding processes with the aid of information, which is derived at the microscopic level. Sliding frictional behaviour of an unlubricated metal couple was studied experimentally and was found to be strongly influenced by operating conditions such as sliding speed and interface temperature for the titanium alloy Ti6Al4V. The different friction regimes observed experimentally are explained using an analytical contact model, which represents the moving system of two interconnected plates at the sliding interface with bonds, which continuously form and rupture during sliding. Moreover, the characterised frictional behaviour, which depends on interface temperature, is used to model numerically the non-linear thermo-mechanical process of linear friction welding of Ti6Al4V.

**Keywords:** continuum model; micromechanical parameterisations; friction coefficient; modelling; stick-slip.

**Reference** to this paper should be made as follows: Vairis, A. and Christakis, N. (2007) 'The development of a continuum framework for friction welding processes with the aid of micromechanical parameterisations', *Int. J. Modelling, Identification and Control*, Vol. 2, No. 4, pp.347–355.

**Biographical notes:** Achilles Vairis received a PhD in Mechanical Engineering from the University of Bristol in 1998. He is currently an Assistant Professor in the Department of Mechanical Engineering of the TEI of Crete in Greece and a Research Fellow with the Centre for Technological Research in Crete. His current research interests include frictional phenomena, modelling and joining technologies.

Nicholas Christakis received a PhD in Physics from UMIST in 1998. He is currently a Visiting Assistant Professor in the Department of Applied Mathematics of the University of Crete and a Research Fellow of the Foundation of Research and Technology, Crete, Greece. His research is in the area of fluid mechanics.

## 1 Introduction

Problems that arise in large-scale industrial processes cannot always be fully understood, due to the complex behaviour of the materials involved, as well as the processes themselves. Many of these problems are solved empirically, yet the solutions lack of generality and do not provide better insight to the causes of the problem. The use of mathematical models is a more systematic scientific approach, which would provide better understanding of the process evolution and would eventually lead to process optimisation.

Recently, a continuum mechanics framework was presented for granular material handling processes in industrial production lines (Chapelle et al., 2004; Christakis et al., 2002, to appear; Wang et al., 2004). It is based on the representation of the material as a continuum and solves for the equations of mass, momentum and energy for the description of material flow under various scenarios (filling-emptying of storage bins, material

transportation on pneumatic conveying lines, material storage under varying environmental conditions). Although this approach provides some information on the flow characteristics it is incomplete, as it lacks essential information on particle interactions with other particles and their environment. In this way, important processes that might lead to poor product quality, such as particle size segregation, particle degradation or particle caking, cannot be modelled, compromising thus the capability of employing such models for industrial process optimisation.

On the other hand, although micromechanical models on their own can adequately reproduce the interactions between particles, thus making possible the simulation of granular material handling processes, they cannot be employed for the simulation of large-scale industrial processes, since the computational cost would be enormous. It has been demonstrated that the next best approach would be to employ experiments and simulations performed at the microscopic level (e.g. Abou-Chakra et al., 2003; Baxter et al., 2002) in order to derive information on the connection between material properties and key flow parameters. This information is parametrised in the form of constitutive laws and utilised in the continuum model, thus making possible the representation of important processes, such as particle segregation, degradation and caking. The models for each process separately were first validated (Chapelle et al., 2004; Christakis et al., 2002; Wang et al., 2004) and then an integrated framework was set up (Chapelle et al., 2005), where all three models were combined in order to develop a toolkit for the simulation of full large-scale processes that involve granular material. The toolkit has been validated and is already in use by industry.

The work performed for granular material sets the trend for the modelling of other complex industrial systems, where continuum mechanics alone is not possible of providing adequate information for the process-system evolution. In this paper, a similar framework will be discussed for the modelling of friction welding, an important process which has serious implications on country economics, as well as machinery life and operation. A continuum model for friction welding will be presented and simulations will demonstrate the capabilities of the model to represent complex material behaviour. Then, a micromechanical analytical model will be discussed, which takes into account the molecular interactions between the formed and ruptured bonds as the welding process evolves and its incorporation in the presented continuum model will be addressed. The aim of this paper is to set a framework within which friction processes will be studied and understood at the microscopic level and appropriate constitutive equations will be derived. These then will be utilised at the macroscale, in order to enable the understanding and the correct representation-modelling of friction welding processes. The approach of utilising information from the microscale in a continuum mechanics framework, is quite novel and is believed to be unique in the context of friction welding processes.

## 2 Friction studies – past and present

The movement of an object along a surface from macro-scale to nano-scale is resisted by forces commonly referred to as friction. These forces are non-conservative and convert the kinetic energy of the moving objects into thermal or mechanical energy, as is evident by the increase in temperature at the rubbing interface or squeaking noises. It is common experience that the necessary force to commence sliding a material is greater than that to maintain motion, and therefore the coefficient of static friction is greater than that of dynamic friction. It has also been observed that the range of values of frictional forces differ by orders of magnitude depending on the length scales of the applications, macroscopic or nanoscopic.

As the French physicist Guillaume Amonton (1699) stated in his empirical law of sliding friction, the friction force is proportional to the normal load, or if expressed mathematically:

$$\text{Friction force} = \text{friction coefficient} \times \text{normal load} \quad (1)$$

In most cases the precise value of the coefficient of friction depends strongly on the experimental conditions under which it is measured. In addition, a second law of friction states that friction force is independent of the apparent area of contact between the two surfaces. Moreover, Charles Augustin de Coulomb stated in his third law of macroscopic friction that friction force is independent of sliding velocity. The coefficient of dynamic friction is expected to be nearly independent of ordinary sliding velocities, and similar behaviour is exhibited for temperature changes, unless phase transformations appear at the interface.

All three laws of friction, although not holding in every condition of stress, temperature, velocity and length scale, have far outlived a number of theoretical attempts to provide a clear explanation of the phenomenon as well as a unified theory for friction in both macroscopic the microscopic levels.

Initial attempts, by Amonton and Coulomb among others, assumed that mechanical interlocking between rigid or elastically deforming asperities are responsible for the frictional force and the consequent mechanical wear and heat generation. This model assumes two bodies which perform both longitudinal and transverse motion at the same time; work is performed by normal load after the upper body has returned to its lowest position, and all of the potential energy is recovered. Unfortunately, macroscopic observations may not be in agreement with this theory as highly polished and smooth surfaces are necessary for cold welding and do not necessarily show low friction. An additional problem for this theory is that adsorbed films change friction by orders of magnitude while maintaining the same roughness of the surface.

A more successful model was proposed in the by Bowden and Tabor (1950) which connected asperities and molecular adhesion. The actual area of contact is much smaller that the apparent area of contact by a factor of 104. Even so, surfaces do rest on each other on asperities, which exhibit local yielding. When surfaces move relative to each other these bonds are damaged while new are

formed, with friction being related to the shear strength of the material. Assuming that normal pressure at the interface is independent of the normal load, the friction coefficient can be estimated as:

$$\text{Friction coefficient} = \frac{\text{shear strength}}{\text{pressure}} \tag{2}$$

Lacking precise and direct measurement methods for the true area of contact, contact mechanics models have been used. The most popular model is one where contact between the two surfaces is represented by two spheres (see e.g. Haile, 1997). The true area of contact is proportional to the normal load to the power of $n$, where $n$ is 2/3 for pure elastic deformation (as in the case of wood and textiles) and 1 for ideal plastic deformation (as in the case of cold-worked steel).

For multiple asperity contact (Greenwood and Williams, 1966), which is closer to the physical situation, a linear relationship was found to be between the true area of contact and normal load for an exponential distribution of asperity heights, which also holds for a Gaussian distribution, and for fractal surface geometries. The significance of this linear relationship is that as the load increases the size of the individual contacts increases as well as the number of the contacts. This concept, which agrees with the Bowden and Tabor model, does apply to a range of materials but contradicts experimental values. Wear rates and ploughing effects are not enough to explain this disparity.

Tomlinson (1929) suggested that phononic or lattice vibration mechanisms could contribute to friction. Vibrations are produced when the mechanical energy necessary for sliding is converted to sound energy which in turn is converted into heat. The phononic approach was verified (Singer and Pollack, 1992) as new experimental and theoretical techniques were available for investigating friction at the micro-scale and the nano-scale. It has been observed that frequently static friction is absent and that solid-liquid and solid-solid interfaces follow a viscous-friction law.

In the macroscopic systems where everything is of different length and time scales, these fundamental energy dissipation mechanisms of phononic and electronic effects have not been clearly identified as yet, as Bowden and Tabor had suspected. In addition, whereas the theoretical prediction that static friction disappears when clean surfaces deform elastically, in practice it does exist, it is quite variable and is always larger than sliding friction.

A related phenomenon is stick-slip friction, where for certain sliding velocities the interface is repetitively sticking and slipping. This phenomenon is responsible for the screeching noises of car braking.

To relate the phenomena of static and stick-slip friction further studies are necessary. As the interfacial geometry changes continuously, friction coefficients are affected and stick-slip occurs. In addition, friction force at an individual asperity level can change with increasing load. These effects may be due to additional adsorbed molecules in the interface.

Unfortunately, existing data and theoretical explanations are strongly dependent on specific conditions, with linking between individual experimental results not being fully established. Realistic laboratory experiments should be well controlled, provide a wealth of information and be relevant to operating machinery. It is estimated that developed countries can conserve up to 1.6% of their Gross National Product by limiting the negative effects of friction and wear, which cause entire mechanical systems to be routinely discarded after certain parts are worn, and by reducing consumed energy used in the manufacture of assemblies (Vairis, 1997b).

In the following sections, the presented framework (experimental – theoretical-numerical) with all relevant assumptions will be discussed in detail, some initial results will be presented and conclusions will be drawn on the potential of the proposed framework to successfully represent friction welding.

## 3 Frictional behaviour experiments

In this section, the experimental procedure is described, which yielded data used in the analysis of the frictional behaviour of the studied alloys.

Typical friction experiments involve pin and disk apparatus or some other mechanism where a pin slides over a given point on a surface intermittently. In the current study, a number of measurements were made under different sliding conditions. Tubular specimens were used with typical dimensions of 22 mm length and radius $r$ of 24 mm and thin walls (1 mm) (see Figure 1). The experimental apparatus (Vairis, 1997a) was instrumented so that the interface coefficient of friction was measured indirectly. The stationary cylindrical specimen was placed in a fixture, which in turn rested on a Kistler piezoelectric transducer which measured directly the normal force exerted by the rotating specimen on the stationary specimen and indirectly the horizontal friction force acting on the specimen. The stationary specimen holder was free to rotate, resting on a thrust bearing that was firmly attached to the force transducer. As the bottom stationary specimen came in contact with the rotating specimen at the top, it would try to rotate as well only to be stopped by the pin. The horizontal reaction force $L$, which was produced by the friction force on the rotating interface, was transmitted to the plate via a lever. Physically, the normal load $N$ applied, the force $L$ produced by the friction force and the friction coefficient $\mu$ can be related by

$$\mu = \frac{\mathrm{Ld/r}}{\mathrm{N}} \tag{3}$$

where $d$ is the distance of the pin attached to the load cell plate from the centre of rotation, transmitting the friction force experienced by the stationary specimen and $r$ the radius of the cylindrical specimen. Alternatively, the coefficient of friction can be related to the stress conditions at the rubbing interface, with

$$\mu = \frac{\tau}{\sigma} \tag{4}$$

where $\tau$ is the shear stress at the rubbing interface and $s$ is the normal stress at the rubbing interface.

**Figure 1** Frictional behaviour experiments apparatus

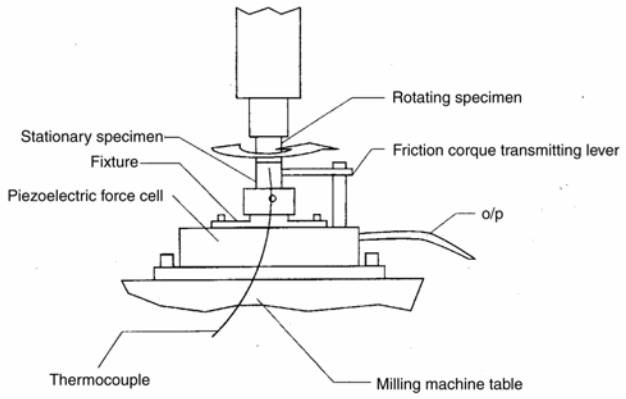


Simultaneous measurements of $N$ and $L$ were used to determine the coefficient of friction experimentally. A thermocouple was used to record the temperature on the stationary specimen, which was spot welded on the outside face of the specimen at a known distance from the interface. The shortening of the specimens was also registered to compensate for the move of the rubbing interface closer to the thermocouple due to wear.

As the recorded temperature was an indirect measure of the actual rubbing interface temperatures, a non-linear finite element model was used to estimate the true temperatures encountered at the interface. The numerical simulation enabled the prediction of the true interface temperature.

Figure 2 shows the relationship between the coefficient of friction and interface temperature for various rubbing velocities for the titanium alloy Ti6Al4V. The alloy studied showed sensitivity to rubbing velocity (480 mm/s). This can be attributed to stick-slip behaviour, as the analytical model shown later suggests. Increasing sliding speed has a direct beneficial effect on thermal softening and simultaneously reduces the time available for surface oxidation.

To verify the applicability of the experimental procedure followed, intermediate values of the friction coefficient, where a large normal load was applied, were compared to the predicted values of the coefficient. The recorded values of the coefficient of friction were within 10% of the values expected by the curves fitted to the experimental data. During these experiments plasticity was not observed, therefore, the relation between temperature and stress was linear, as is expected by theory (Rabinowicz, 1995).

Results obtained in the frictional behaviour experiments are similar to experimental values reported in literature. In particular (ASM, 1992) the dynamic coefficient of friction of Ti6Al4V is reported to be 0.4 and 0.31 in different experimental arrangements. This is not in disagreement with the average room temperature value of 0.43 recorded here. A more detailed presentation of the experiment may be found in Vairis (1997b).

## 4 Linear friction welding modelling

The characterised frictional behaviour of Ti6Al4V was used to model numerically the process of linear friction welding (Vairis, 1997b; Vairis and Frost, 2000). Friction is used by the linear friction welding process as a means to clear the rubbing interface of oxides and anomalies, while at the same time generating enough heat for the material at the heat affected zone to reach incipient yield conditions. Due to high temperatures reached, which are below melting temperatures, the interface deforms plastically and allows material to be extruded from the sides of the rubbing interface and finally the two objects are joined together once rest is reached.

**Figure 2** Frictional behaviour of Ti6Al4V

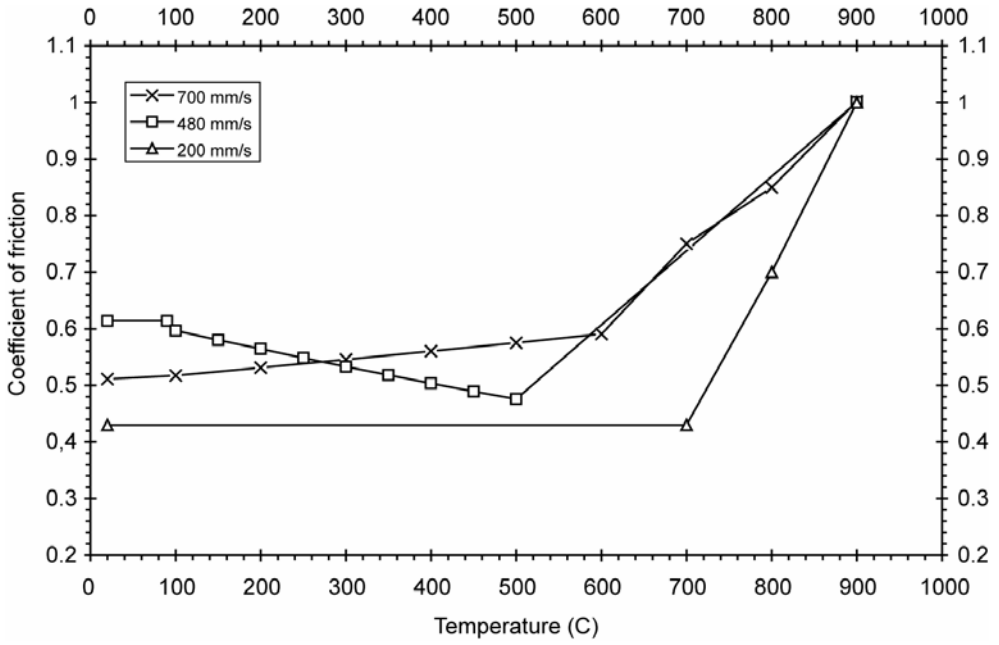

The numerical modelling of the welding process had a number of features. The first was thermal-mechanical coupling, as the process is separated into a mechanical and a thermal problem to be solved in parallel during every time step in the analysis. Another feature of the analysis is material non-linearity, as material properties affect considerably the accuracy of the predictions, where temperature dependent material properties were used to accurately represent the process including the use of viscoplastic constitutive laws for the case of Ti6Al4V. A third feature of the process modelling were the complex thermal boundary conditions, of heat conduction from the rubbing interface to the bulk of the specimens, convection losses to the surrounding air, radiation losses due to the high temperatures reached (of the order of 1000°C) and friction flux as a result of movement between the two specimens. Complex mechanical boundary conditions complicated further the analysis as there was variation with time of both the surface contact area and the frictional parameters, with the friction coefficient changing with temperature as experiments have shown.

Numerical simulations were performed using the finite element software ELFEN. The process model of linear friction welding of similar metals can be reduced to half of the original model size, by defining one of the two specimens as rigid, leaving the other object as deformable body. Although frictional heat is generated between deformable and rigid surfaces, temperature rises are effected only on the deformable body, thus reducing the processing time. A total of 764 isoparametric plane stress triangular elements were employed to discretise the two blocks. The top object was set as deformable, while the one at the bottom was set as rigid in an effort to reduce the problem and shorten the analysis time.

The bottom object was constrained in the $x$ and $y$ directions along the bottom face of it. The nodes at the top face of the top block were coupled to move together in both degrees of freedom, as these were the nodes where the oscillatory movement and the friction pressure were applied on. The constraint for the thermal model was to set an initial temperature of 20°C for both objects. The mechanical loads applied were the normal pressure on the top face of the top block, and a prescribed displacement at the corner node of the same face. The displacement changed with time to a sinusoidal function at the required frequency of oscillation. Loading for the thermal analysis included convection and radiation losses.

Non-linear mechanical and thermal material properties were used, the values of which depended on temperature. The power law viscoplastic option was employed to represent the material flow rule. The viscoplastic flow rate can be associated to stress conditions in the finite element formulation through the equation:

$$\dot{\tilde{\varepsilon}}^{\mathrm{vp}} = \gamma \left[ \frac{\tilde{\sigma} - \tilde{\sigma}_y}{\tilde{\sigma}_y} \right]^N \tag{5}$$

From experimental data (Chaudhury and Zhao, 1992) at the temperatures and strain rates most likely to be encountered in linear friction welding of Ti6Al4V the fluidity parameter $\gamma$ is set to $2.75 \times 10^{-4}$ and the exponent $N$ to 4. Contact between the two sliding surfaces was modelled with a series of contact sets, commonly known as slidelines. As the surfaces were in sliding contact, the friction law of Coulomb was used.

Frictional work is generated only when parts of the contact surfaces are in contact. To define the mechanical behaviour of the slidelines a number of associated data are necessary, such as the friction coefficient, taken form the experiments, and parameters for the numerical simulation of deformable bodies.

In order to verify the accuracy of the finite element model developed, the temperature at a known position and shear stress conditions need to be identified.

The temperature was recorded using a chromel-alumel thermocouple embedded in a blind hole in the stationary specimen at a predetermined depth.

As can be seen (see Figure 3) the temperature prediction of the finite element model closely agrees with the one recorded up to 4 sec into the process, where they start to deviate. The recorded temperature in the experiment does reach a plateau, before declining. The reason for this lies in the complex metalworking

**Figure 3** Comparison between experimental data and temperature prediction of the finite element model

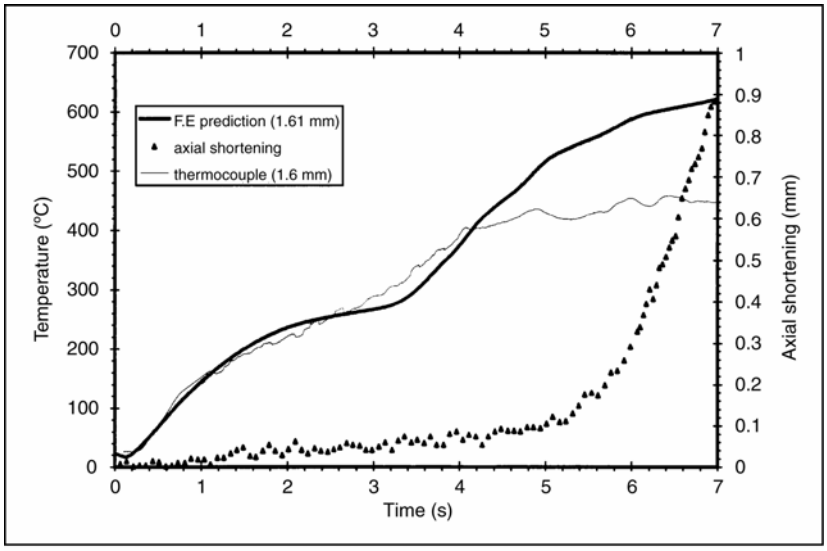

conditions present at the rubbing interface. During the first seconds of the process, material is removed from the interface due to wear and frictional heat raises the temperature at the interface. As material yields locally, either it is extruded from the sides of the specimen, or moves into the hole where the thermocouple is situated. This causes the thermocouple to move away from the interface, where it registers lower temperatures at an unknown distance from the rubbing interface if not damaged.

The finite element model prediction for a node in the middle of the rubbing interface (see Figure 4) predicts that the temperature will not rise above 900°C and that it will remain steady around that temperature. Although data from thermocouples corroborate the fact that temperatures at the interface should not have exceeded the beta transus temperature of 995°C, metallurgical observations indicated the opposite as acicular alpha was identified in the weld interface. An explanation for this could be that thermocouple measurements can give underestimates of the actual conditions due to the limited control over the thermal inertia, the response time and the positioning of the junction in the specimen.

**Figure 4** Finite element analysis temperature prediction at rubbing interface

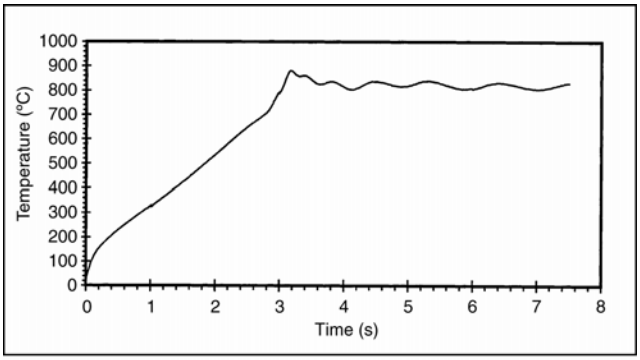


The finite element model predicted a shear force of 1500 N at 5 sec into the process, while at the same time the average experimental value was 1425 N, a difference of 5%.

The finite element model studied the initial stages of linear friction welding of Ti6Al4V and the predicted temperatures were in reasonable agreement with the ones recorded in the experiments by thermocouples close to the rubbing interface. This agreement indicates consistency between theory and experiment.

## 5 Analytical contact model

The irreversible phenomenon of friction originates from the formation and fracture of junctions at the microscopic level formed between the rubbing surfaces, with different regimes relative to sliding velocity. In particular the stick-slip regime is associated with cooperative rupture of bonds.

The microscopic model that attempts to relate to macroscopic surfaces motion was reported in the literature (Filippov et al., 2004). Two rigid surfaces are connected by junctions that spontaneously break and form upon contact. The junctions are assumed to behave as elastic springs with a force constant κ and a rest length l (0). A spring of constant K is exerting the necessary force to move the top surface at a constant velocity *V*. The equation of motion of the driven surface is

$$M\ddot{X} + \eta\dot{X} + F_{\mathrm{b}} + K(x - Vt) = 0 \tag{6}$$

where the force due to the interaction between the junctions and the driven surface is $F_{\mathrm{b}}$ and $\eta$ is the damping coefficient. The force $F_{\mathrm{b}}$ is given by the equation:

$$F_{\mathrm{b}} = \sum_{i=1}^{N} q_i f_i^{(x)} \tag{7}$$

where $q_i$ indicates the state of the junction (with $q_i$ = 1 for the formed junction and $q_i$ = 0 for the breached junction).

The elastic force $f_i$ from the junction formed is given by Hooke's law, with l being the length of the junction:

$$f_i = \mathrm{k}\left[l_i - l^{(0)}\right] \tag{8}$$

The top surface is continuously forming junctions that hinder sliding and extend. At the same time it is breaking junctions with the bottom stationary surface, similar to spring detachment that assists sliding.

The model junctions extend and contract as the two surfaces slide on each other, with the dynamics of this being represented by velocity:

$$\dot{x}_i = q_i\dot{X} - \lambda\left(1 - q_i\right)x_i \tag{9}$$

where the extension-compression rate of the junctions is considered to be equal to the relative velocity of the two surfaces. The relaxation constant $\lambda$ characterises the approach of a junction to its equilibrium length. This action is different for each junction, as is the length of the junction and the resulting elastic forces are different for each individual junction.

The state of the individual junction $q_i$ can be described in time in terms of the existing number of junctions, the number of junctions formed and the junctions fractured:

$$\begin{aligned} q_i(t + \Delta t) &= q_i(t) - q_i(t)\theta\left(\xi_i - \Delta t k_{\mathrm{off}}\right) \\ &+ \left[1 - q_i(t)\right]\theta\left(\xi_i - \Delta t k_{\mathrm{on}}\right) \end{aligned} \tag{10}$$

where $\Delta t$ is the time step, $\xi_i$ is a random variable in the interval (0,1) and $\theta(z)$ is the Heaviside step function for the description of the stochastic creation and fracture of a junction that occurs for $\xi_i < \Delta t k_{\mathrm{off(on)}}$. The rate of creation and fracture of junctions is $k_{\mathrm{on}}$ and $k_{\mathrm{off}}$, respectively.

The junction fracture can be regarded as a thermally assisted escape from a state over an activation barrier $\Delta E(l_i)$, which is dependent on the length of the junction spring and decreases as the elastic energy increases with increasing junction length. Junctions can be of two types: weak junctions where the junction energy is slightly larger than $k_{\mathrm{B}}T$, with $k_{\mathrm{B}}$ being the Boltzmann constant and strong

junctions, where the energy is much larger than $k_B T$. In the case of a weak junction the time-dependent fracture rate is:

$$k_{\text{off}}\left(l_i\right) = k_0 \exp\left(\beta f_i \Delta x\right) \tag{11}$$

where $\beta = 1/k_B T$ and $\Delta x$ is the difference between the maximum and minimum of the reaction potential. As can be seen, a steady increase in the attracting force produces a small constant bias which reduces the potential barrier. In the case of a strong junction:

$$k_{\text{off}}\left(l_i\right) = k_0\left(1-\frac{f_i}{f_c}\right)^{1/2} \exp\left\{-\beta\left[U_0\left(1-\frac{f_i}{f_c}\right)^{3/2} - U_0\right]\right\} \tag{12}$$

where $k_0$ is the spontaneous rate of junction fracture when there is no external force present, $U_0$ the depth of the potential, $f_c$ the critical force at which the potential barrier disappears and is released in the absence of thermal fluctuations. This equation assumes that at a high potential barrier a junction fractures preferentially when the junction is close to slipping.

The junction creation or reattachment, is characterised by the rate $k_{on}$, which is assumed for simplicity to remain unaffected by the junction length, but depends on the age of the contact $\tau$. This age $\tau$ is the time that the free end of the junction is exposed to the moving interface. The rate of junction creation is dependent on the time difference between the age of the junction $\tau_0$ and the present time $\tau - \tau_0$:

$$k_{\text{on}} = k_{\text{on}}^0\left[\frac{\tau-\tau_0}{\Delta\tau}\right] \tag{13}$$

with $k_{\text{on}}^0$ being the rate of junction creation for a stationary contact, $g$ being a modified stepwise function (where $g = 0$ for junction age $\tau << \tau_0$, $g = 1$ for $\tau > \tau_0$). Contact time $\tau$ is inversely proportional to sliding velocity, with the contact being related to the typical length scale of the contact $\alpha$ by the equation:

$$\tau = \frac{\alpha}{\dot{X}} \tag{14}$$

The characteristic time-scale $\tau_0$, necessary for junction creation, is used to define a critical velocity:

$$V_0 = \frac{\alpha}{\tau_0} \tag{15}$$

Above this velocity junctions cannot be formed. This is necessary in order to accurately represent stick-slip conditions.

Applying the model to a large number of junctions ($N > 300$), where the measurable frictional forces are proportional to $N$, a clear picture emerges of three different frictional behaviour regimes.

There are two sliding regimes with a stick slip region between them. These frictional behaviour regimes can be recognised (Figure 5) where the time-averaged maximal and minimal values of the spring forces are related to sliding velocity through the equation:

$$F = K\left(X - V_t\right) \tag{16}$$

The maximal and minimal values of the spring forces coincide in the sliding regime, but differ in the stick-slip regime, clearly demonstrating this stick-slip behaviour (see Figure 5a). This dynamical behaviour has been observed both in the macroscopic, as the previously described experiments-macroscopic simulations show and in the microscopic scale.

The three frictional regimes exhibit different behaviour, with different mechanisms being responsible for the frictional behaviour observed. The low sliding velocity regime represents a state where thermal bond dissociation determines junction fracture rather than shear-induced stress. This regime behaviour correlates with the observation that the value of static friction depends on the time scale. This region is consistent with atomic scale stick-slip motion of individual junctions. The low sliding velocity frictional regime, which is characterised by energy dissipation, is dependent on the fracture and the subsequent relaxation of junctions, rather than on viscous dissipation, as Figure 5(b) shows.

In the stick-slip region, at an intermediate sliding velocity $V >> V_c$, the processes of spontaneous and

**Figure 5** Velocity dependence of time-averaged frictional forces in the case of weak bonds. (a) Maximal (closed circles)and minimal (open circles) spring forces calculated within the microscopic model for weak bonds. (b) The net kinetic friction (bold line), rupture (dashed line) and viscous (thin line) components of the friction force

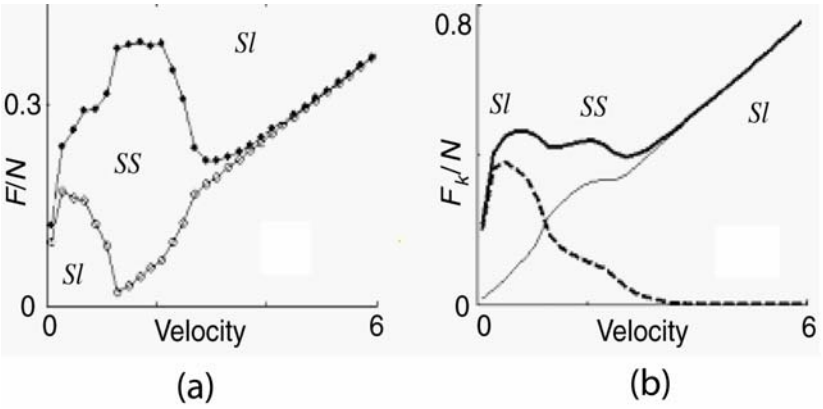


*Note*: (Sl and SS indicate sliding and stick-slip regions correspondingly).

*Source*: Filippov et al. (2004).

shear-induced bond dissociation compete and produce an erratic stick-slip motion. The stick-slip region has a more regular behaviour as velocity increases $V_0 > V >> V_c$. Junction fracture is controlled by the effect of shear stress on the activation barrier. At this time the fraction of intact junctions decreases with a similar decrease of the fracture contribution to the energy dissipation. The net kinetic friction is relatively insensitive to the sliding velocity in this regime as the effect of the diminishing fractures contribution is counterbalanced by the viscous component of the energy dissipation. The system shows a cooperative behaviour, where as the number of breaking bonds increases the force on the remaining bonds increases and bond rupture synchronises, thus producing a more consistent stick-slip behaviour. There is a correlation between macroscopic frictional properties and a collective behaviour of microscopic bonds (Budakian and Putterman, 2000).

The high sliding velocity region shows a transition from stick-slip behaviour to smooth sliding. Bond formation becomes impossible due to the short contact time, $\tau < \tau_0$. Frictional force in this regime is completely determined by viscous dissipation:

$$F = \eta V \tag{17}$$

## 6 Conclusions

The frictional behaviour experiments with dry sliding demonstrated dependence on interface temperature, as well as on rubbing velocity (see Figure 2). Although this behaviour is not predicted by the original theories of macroscopic friction, the rubbing velocity dependence of friction coefficient can be explained by an analytical microscopic model, where two plates are interconnected at the sliding interface with junctions that continuously form and rupture during sliding. This model demonstrated qualitatively a dependence of frictional behaviour on sliding speed, with stick-slip phenomena being responsible for this. It is suggested that the dependence on temperature can be attributed to similar mechanisms of junction formation and fracture and could be further explored by its incorporation in the analytical contact model. In this way, appropriate constitutive laws will be developed, at the microscale, which will assist the macroscopic continuum model in more accurately predicting frictional behaviour during linear friction welding for a range of materials and a range of conditions. Currently, work is under way for the derivation of such laws, which will parameterise the frictional behaviour dependence on sliding velocity, as well as interface temperature.

As has already been discussed, recent studies have shown a promising trend for the modelling of large-scale engineering processes where complex micromechanical phenomena play an important role, with the development of a continuum framework assisted by micromechanical parameterisations (see e.g. Chapelle et al., 2005). The development of a similar framework in the area of linear friction welding would be of great importance in the engineering community, as it will assist in the better understanding of material frictional behaviour and will enable the optimisation of linear friction welding processes. The application of such a framework in friction welding processes is believed to be unique and as such, might initially encounter potential difficulties when conducting experiments at the microscale.

## Acknowledgements

The authors wish to thank Dr I. Tsagrakis of the Department of Applied Mathematics of the University of Crete for his constructive comments during the writing of this paper.

## References

Abou-Chakra, H., Tüzün, U., Bridle, I., Leaper, M., Bradley, M.S.A. and Reed, A.R. (2003) 'Assessing the potential of a fine powder to segregate using laser diffraction and sieve particle size measuring techniques', *Advance Powder Technology*, Vol. 14, No. 2, pp.167–177.

Amontons, G. (1699) 'De la resistance cause dans les machines', *Mem.Del'Academie Royale*, A, pp.275–282.

ASM Handbook, (1992) *Friction, Lubrication and Wear Technology*, USA: ASM.

Baxter, J., Gröger, T., Abou-Chakra, H., Tüzün, U., Christakis, N., Patel, M.K. and Cross, M. (2002) 'Micro-mechanical parameterisation for continuum modelling of granular material using the discrete element method', in H.A Mang, F.G. Rammerstorfer and J. Eberhardsteiner (Eds). *Proceedings of the Fifth World Congress on Computational Mechanics* (WCCM), Austria: Vienna University of Technology, ISBN 3-9501554-0-6.

Bowden, F.P. and Tabor, D. (1950) *Friction and Lubrication of Solids*, England: Oxford University Press.

Budakian, R. and Putterman, S.J. (2000) 'Correlation between charge transfer and stick-slip friction at a metal-insulator interface', *Physical Review Letters*, Vol. 85, No. 5, p.1000.

Chapelle, P., Abou-Chakra, H., Christakis, N., Bridle, I., Patel, M.K., Baxter, J., Tüzün, U. and Cross, M. (2004) 'Numerical predictions of particle degradation in industrial scale pneumatic conveyors', *Powder Technology*, Vols. 143/144, pp.321–330.

Chapelle, P., Christakis, N., Wang, J., Strusevich, N., Patel, M.K., Cross, M., Abou-Chakra, H., Baxter, J. and Tüzün, U. (2005) 'Application of simulation technologies in the analysis of granular material behaviour during transport and storage', *Proceedings of the I.Mech.E., E: Journal of Process Mechanical Engineering*, Vol. 219, No. 1, pp.43–52.

Chaudhury, P. and Zhao, D. (1992) *Atlas of formability : Ti6Al4V ELI*, Johnstown, USA: National Center for Excellence in Metalworking Technology.

Christakis, N., Chapelle, P. and Patel, M.K. (to appear) 'Analysis and modelling of heaping behaviour of granular mixtures', *Advanced Powder Technology*.

Christakis, N., Patel, M.K., Cross, M., Baxter, J., Abou-Chakra, H. and Tüzün, U. (2002) 'Prediction of segregation of granular material with the aid of PHYSICA, a 3D unstructured, finite volume modeling framework', *Int. J. Numerical Methods in Fluids*, Vol. 40, pp.281–291.

Filippov, A.E., Klafter, J. and Urbakh, M. (2004) 'Friction through dynamical formation and rupture of molecular bonds', *Physical Review Letters*, Vol. 92, p.135503.

Greenwood, J.A. and Williams, J.B. (1966) 'Contact of nominally flat surfaces', *Proceedings Royal Society London*, A 295, p.300.

Haile, J.M. (1997) *Molecular Dynamics Simulation: Elementary Methods*, USA: John Wiley & Sons.

Rabinowicz, E. (1995) *Friction and Wear of Materials*, USA: John Wiley &Sons.

Singer, I.L. and Pollack, H.M. (1992) *Fundamentals of Friction: Macroscopic and Microscopic Processes*, Kluwer, Dordrecht.

Tomlinson, G.A. (1929) 'A molecular theory of friction', *Philos Magazine*, Vol. 7, No. 7, pp.905–939.

Vairis, A. (1997a) 'Investigation of frictional behaviour of various materials under sliding conditions', *European Journal of Mechanics A/Solids*, Vol. 16, No. 6, pp.929–945.

Vairis, A. (1997b) 'High frequency linear friction welding', PhD thesis, England: University of Bristol.

Vairis, A. and Frost, M. (2000) 'Modelling the linear friction welding of titanium blocks', *Materials Science Engineering*, A292, pp.8–17.

Wang, J., Christakis, N., Patel, M.K., Leaper, M.C. and Cross, M. (2004) 'A computational model of coupled heat and moisture transfer with phase change in granular sugar during varying environmental conditions', *Numerical Heat Transfer*, Part A, Vol. 45, No. 8, pp.751–776.